

The *chianti* zebrafish mutant provides a model for erythroid-specific disruption of *transferrin receptor 1*

Rebecca A. Wingert, Alison Brownlie, Jenna L. Galloway, Kimberly Dooley, Paula Fraenkel, Jennifer L. Axe, Alan J. Davidson*, Bruce Barut, Laura Noriega, Xiaoming Sheng, Yi Zhou, Tübingen 2000 Screen Consortium† and Leonard I. Zon*,‡

Department of Hematology/Oncology, Children's Hospital, Harvard Medical School, Boston, MA 02115, USA

*Howard Hughes Medical Institute

†A list of the members of the Consortium and their affiliations is provided at the end of the manuscript

‡Author for correspondence (e-mail: zon@enders.tch.harvard.edu)

Accepted 20 October 2004

Development 131, 6225–6235

Published by The Company of Biologists 2004

doi:10.1242/dev.01540

Summary

Iron is a crucial metal for normal development, being required for the production of heme, which is incorporated into cytochromes and hemoglobin. The zebrafish *chianti* (*cia*) mutant manifests a hypochromic, microcytic anemia after the onset of embryonic circulation, indicative of a perturbation in red blood cell hemoglobin production. We show that *cia* encodes *tfr1a*, which is specifically expressed in the developing blood and requisite only for iron uptake in erythroid precursors. In the process of isolating zebrafish *tfr1*, we discovered two *tfr1*-like genes (*tfr1a* and *tfr1b*) and a single *tfr2* ortholog. Abrogation of *tfr1b* function using antisense morpholinos revealed that this paralog was dispensable for hemoglobin production in red cells. *tfr1b* morphants exhibited growth retardation and brain necrosis, similar to the central nervous system defects

observed in the *Tfr1* null mouse, indicating that *tfr1b* is probably used by non-erythroid tissues for iron acquisition. Overexpression of mouse *Tfr1*, mouse *Tfr2*, and zebrafish *tfr1b* partially rescued hypochromia in *cia* embryos, establishing that each of these transferrin receptors are capable of supporting iron uptake for hemoglobin production in vivo. Taken together, these data show that zebrafish *tfr1a* and *tfr1b* share biochemical function but have restricted domains of tissue expression, and establish a genetic model to study the specific function of *Tfr1* in erythroid cells.

Key words: Zebrafish, Hematopoiesis, Transferrin receptor, Iron, Gene duplication

Introduction

Iron acquisition by developing erythroid cells is necessary to produce hemoglobin, which allows red blood cells to deliver oxygen to body tissues in exchange for carbon dioxide. The processes of iron uptake and intracellular transport are precisely regulated to protect cells from the toxic effects of free iron (Hentze et al., 2004). In vertebrates, the major pathway by which all cells obtain iron occurs through the interaction of transferrin receptor 1 (*Tfr1*) with its ligand transferrin (*Tf*) (Aisen, 2004; Andrews, 2000). *Tfr1* is a type II membrane protein that facilitates iron uptake by binding to the iron carrier *Tf*, a plasma glycoprotein that shuttles iron absorbed from the diet. When bound, the *Tf/Tfr1* complex is internalized by clathrin-mediated endocytosis. Acidification of the endosome compartment by proton pumps causes the release of iron from *Tf*. Iron is subsequently delivered to the cell cytoplasm through the action of the transmembrane protein divalent metal transporter 1 (*DMT1*), which transports iron out of the endosome by means of a proton-coupled process. In erythroid cells, most iron is carried to the mitochondria, where it is incorporated with protoporphyrin to produce heme. Recycling of the endosome restores the apo-*Tf/Tfr1* complex to the cell surface, with the pH of the external milieu causing the release

of apo-*Tf*, such that both *Tfr1* and *Tf* are available for repeated cycles of use.

Tfr1 is highly expressed on differentiating erythrocytes, reflecting their substantial iron requirement to support hemoglobin synthesis (Ponka and Lok, 1999). The murine knockout of *Tfr1* established that it was required for erythropoiesis and embryonic development (Levy et al., 1999). Mice homozygous for a null *Tfr1* allele died of anemia before embryonic day (E) 12.5, and displayed marked growth retardation, edema and signs of tissue necrosis. *Tfr1*^{−/−} mice also showed neurologic abnormalities, including kinking of their neural tubes and increased neuronal apoptosis. In addition, *Tfr1*^{+/−} embryos evinced hypochromic, microcytic erythrocytes, consistent with iron deficiency. Analysis of chimeric mice generated with *Tfr1*^{−/−} embryonic stem cells illustrated that *Tfr1* was required postnatally for adult erythropoiesis and lymphopoiesis, as *Tfr1*^{−/−} cells did not contribute to the bone marrow, spleen or thymus (Ned et al., 2003). Conversely, *Tfr1*^{−/−} cells did incorporate into all non-hematopoietic tissues, indicating that other pathways of iron uptake were sufficient to permit their survival (Ned et al., 2003).

In addition to *Tfr1*, mammals also possess transferrin receptor 2 (*Tfr2*), a type II membrane protein similar to *Tfr1*.

Tfr2 is highly expressed in liver hepatocytes and erythroid precursor cells, and can facilitate Tf-bound iron entry in vitro, but its function remains poorly understood (Fleming et al., 2000; Fleming et al., 2002; Kawabata et al., 1999; Kawabata et al., 2001; Trinder and Baker, 2003). Furthermore, while alternative mechanisms to Tf/Tfr1-mediated iron acquisition have been characterized in a variety of mammalian cell lines, their in-vivo roles remain to be elucidated. These include direct uptake of non-Tf-bound iron (NTBI) (Baker et al., 1998; Goto et al., 1983; Hodgson et al., 1995; Inman and Wessling-Resnick, 1993; Kaplan et al., 1991; Sturrock et al., 1990), Tfr1-independent uptake of Tf-bound iron (Chan et al., 1992; Thorstensen et al., 1995), and receptor-mediated uptake of ferritin (Gelvan et al., 1996; Konijn et al., 1994; Leimberg et al., 2003; Meyron-Holtz et al., 1999). Recently, the soluble protein 24p3/neutrophil gelatinase-associated lipocalin (Ngal) was found to deliver iron to developing mammalian kidney epithelial cells, with a pattern of cell binding and intracellular trafficking independent from that of the Tf/Tfr1, and may present one avenue for the cellular distribution of NTBI (Yang et al., 2002).

The inability of erythrocytes to obtain adequate iron for hemoglobin synthesis, as well as defects in heme or globin production, causes hypochromic, microcytic anemias in humans. While low dietary iron or blood loss is most frequently the underlying cause, inherited mutations in any number of genes required for hemoglobin synthesis have been attributed to such anemias (Andrews, 1999). We have utilized the zebrafish *Danio rerio* as a genetic model to study hemoglobin production during vertebrate erythropoiesis (Brownlie and Zon, 1999; Wingert and Zon, 2003). Zebrafish hematopoietic screens have resulted in the identification of nine complementation groups that display hypochromic, microcytic anemia: *chardonnay*, *chianti*, *frascati*, *gavi*, *montalcino*, *sauternes*, *shiraz*, *weissherbst* and *zinfandel* (K.D., P.F., R.A.W. and L.I.Z., unpublished) (Haffter et al., 1996; Ransom et al., 1996). *chardonnay* (*cdy*) has a mutation in *Dmt1* (Donovan et al., 2002). The *weissherbst* (*weh*) mutant is unable to obtain maternal iron yolk stores due to a defect in *ferroportin 1* (*Fpn1*), a transmembrane protein required to transport iron from the yolk into embryonic circulation (Donovan et al., 2000). The mutant *sauternes* (*sau*) has a defect in the enzyme aminolevulinate synthase-2 (Alas2), which functions at the first step in heme biosynthesis (Brownlie et al., 1998). Lastly, the *zinfandel* (*zin*) mutation has been mapped to the major globin locus, suggesting that *zin* results from disrupted globin function (Brownlie et al., 2003).

We report here the characterization of the *chianti* (*cia*) mutant phenotype and the cloning of the *cia* gene. We show that *cia* encodes an erythroid-specific isoform of *transferrin receptor 1* (*tfr1a*) that is solely required for iron acquisition by differentiating erythrocytes. We found that zebrafish have undergone and retained a duplication of *Tfr1* during teleost evolution, adding *tfr1a* and *tfr1b* to the growing list of gene duplicates in teleosts. To determine the function of zebrafish *tfr1b*, we utilized a morpholino knockdown approach and found that *tfr1b* is not required for erythropoiesis, but rather necessary for normal development of non-hematopoietic cells. These findings establish that the combined functions of *tfr1a* and *tfr1b* in zebrafish embryos recapitulate the role of mammalian *Tfr1*. Thus the *cia* mutant provides a useful genetic

model to study the role of Tfr1 in erythropoiesis in the absence of other developmental defects.

Materials and methods

Zebrafish strains and maintenance

Zebrafish were maintained (Westerfield, 1993) and staged as described (Kimmel et al., 1995). *cia^{tu25f}* was generated on the Tübingen (Tü) strain in a large-scale ENU mutagenesis screen (Haffter et al., 1996; Ransom et al., 1996), and crossed to standard wild-type AB for maintenance. *cia^{hp327}*, *cia^{hs019}*, and *cia^{tu089}* were obtained by screening for zebrafish with hypochromia in a second large-scale ENU mutagenesis screen (K.D. and L.Z., unpublished); these alleles were generated and maintained on the Tü background. Matings with *cia^{tu25f}* homozygotes and linkage analysis were used to assemble the *cia* complementation group.

o-dianisidine staining, in-situ hybridization and histological analysis

Detection of hemoglobin by *o*-dianisidine was performed as described (Ransom et al., 1996). We performed whole-mount in-situ hybridization with digoxigenin-labeled RNA probes as described (Thompson et al., 1998). Synthesis of *βe1 globin* probe was performed as described (Brownlie et al., 1998). Antisense and sense *tfr1a* and *tfr1b* probes were synthesized from the respective cDNA clones in pGEM-T easy vector. Adult peripheral blood and kidney tissue samples were isolated and Wright-Giemsa stained as described (Ransom et al., 1996; Brownlie et al., 1998).

Meiotic mapping

Genetic mapping strains were created by mating *cia* AB or Tü heterozygotes to the polymorphic Dar or WIK strains. Embryos were collected from pairwise matings of mapping strain *cia* heterozygotes, and scored at 72 hours post fertilization (hpf) for hypochromia. Genomic DNA extraction from individual embryos and bulk segregant analysis were performed as described (Zhang et al., 1998) using primers designed to SSLP markers obtained from the Massachusetts General Hospital Zebrafish Server website (<http://zebrafish.mgh.harvard.edu>) and synthesized by Invitrogen.

Isolation of zebrafish Tfr genes, radiation hybrid mapping and mutation analysis

A 329 bp fragment of zebrafish *tfr1a* was isolated from zebrafish kidney cDNA library using degenerate primers, 5'-TACACMCCWG-GMTTCCC-3' (forward) and 5'-CCTGGRCCCCATGCATCCC-TCTG-3' (reverse). This fragment was used to screen zebrafish kidney cDNA gridded filters, which obtained partial clones of *tfr1b*. For each *tfr1*, a combination of 5' and 3' rapid amplification of cDNA ends (RACE) was used to determine the entire cDNA sequence; full-length clones were then obtained by RT-PCR from 36 hpf embryos, using 5'-ATGGATCAAGCCAGGACAACC-3' (forward) and 5'-CTAAA-GAGGTGAGCTGAAG-3' (reverse) primers for *tfr1a*, and 5'-ATG-GCAGGAACAATTGGTCAA-3' (forward) and 5'-CTAGATTT-CGTTGTCCAGGGA-3' (reverse) for *tfr1b*. A partial fragment of *tfr2* was cloned using online genome sequence data, and the open reading frame determined by 5' RACE; a full-length clone was obtained by RT-PCR from 36 hpf embryos using 5'-ATGATGGACTCGGTCA-CAGGA-3' (forward) and 5'-CTACAGCGGGTTGTTCGATGTT-3' (reverse). Radiation hybrid mapping was done with the following forward and reverse PCR primers: *tfr1a*, 5'-CAACAACAT-CCTCGTTTCAG-3' and 5'-CTCTGGACCCCGATCACC-3'; *tfr1b*, 5'-GCTTCGACATCGACCAGGTGC-3' and 5'-GCACCTGAAA-TGGGAGC-3'; and *tfr2*, 5'-CCCATCAGCAGATGAACCAACGAA-3' and 5'-ACATAGGTGTGTTTACCGTTTTCC-3'. Mutation analysis was done by isolating cDNA from each *cia* allele at 36 hpf. *tfr1a* was amplified using the primers above, subcloned into pGEM-T Easy vector (Promega), and clones sequenced to determine the mutations.

cdNA overexpression constructs and morpholino designs

Full-length *tfr1a* and *tfr1b* cDNAs were subcloned into the pCS2+ vector and mRNA synthesized using SP6 mMessage mMachine (Ambion). *mtfr1* and *mtfr2* cDNA clones were a gift from Vera Sellers (Children's Hospital, Boston), and were subcloned into pCS2+. For expression in zebrafish *cia^{tu089}* embryos, approximately 500–600 pg of synthetic mRNA encoding *tfr1a*, *tfr1b*, *mtfr1* or *mtfr2* was injected into 1–4-cell stage embryos.

Two morpholino antisense oligonucleotides targeting the *tfr1a* transcript were obtained from Gene-Tools: *tfr1a*-MO1 (5'-AGATGG-TTGTCCTGGCTTGATCCAT-3') was designed to the predicted start codon (underlined); *tfr1a*-MO2 (5'-ACACCTTCGAGTGGAC-GAAGTAACAC-3') was designed to the splice donor of exon 13. Embryos were injected with 1 nl of either *tfr1a*-MO1 at 0.1 mg/ml or with *tfr1a*-MO2 at 1.5 mg/ml; to rescue *tfr1a*-MO1, embryos were co-injected with 500 pg of *tfr1a* cRNA. Morpholinos designed against the *tfr1b* transcript were as follows: *tfr1b*-MO1 (5'-CCAATTG-TTCCTGCCATGGGATCTG-3') was designed against the predicted start codon (underlined), *tfr1b*-MO2 (5'-AACAAAACCTACCATT-CTGGAAAC-3') and *tfr1b*-MO3 (5'-GCGGCTGTTTACCTATTA-ACAGAGG-3') were designed against the respective splice donor and acceptor sites between exons 1 and 2. Embryos were injected with 1 nl of *tfr1b*-MO1 at 1.25 mg/ml or co-injected with *tfr1b*-MO1/MO2 at 0.5 mg/ml each; to rescue *tfr1b*-MO1, embryos were co-injected with 300 pg of *tfr1b* mRNA.

Iron-dextran microinjection assays

Intravenous iron injection at 48 hpf was performed as previously described (100 mg/ml, Sigma), such that each embryo received approximately 100 ng iron-dextran (Donovan et al., 2000). For 1-cell injections, iron-dextran was diluted to 10 mg/ml, and embryos injected with approximately 10 ng iron-dextran.

GenBank accession numbers

Zebrafish *tfr1a*, AY649363; zebrafish *tfr1b*, AY649364; and zebrafish *tfr2*, AY649365.

Results

Phenotypic analysis of the *cia* mutant

Four autosomal recessive alleles of the *cia* mutant, *cia^{hp327}*, *cia^{hs019}*, *cia^{tu089}* and *cia^{tu25f}*, were obtained in large-scale ENU

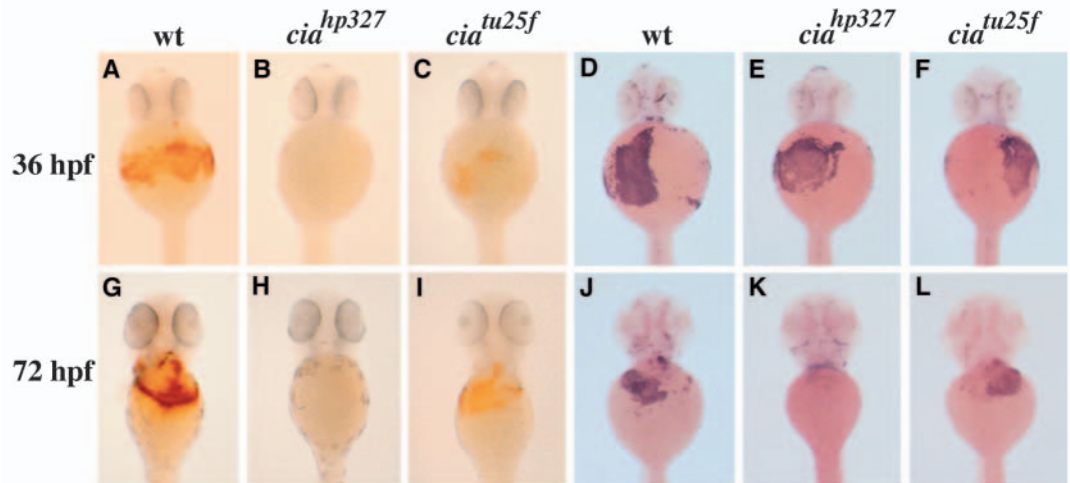
mutagenesis screens for zebrafish with defects in embryogenesis (K.D. and L.Z., unpublished) (Haffter et al., 1996; Ransom et al., 1996). The *cia* alleles displayed a phenotypic range with regard to the onset and severity of hypochromic anemia. Hypochromia was assessed by staining for hemoglobin with *o*-dianisidine, and red cell number was evaluated by in-situ hybridization for *βe1 globin* expression. Hypochromia was first evident at 36 hpf, when *cia^{tu25f}* embryos exhibited a marked decrease in the number of cells stained with *o*-dianisidine, while *cia^{hp327}*, *cia^{hs019}* and *cia^{tu089}* had no detectable *o*-dianisidine-positive cells (Fig. 1A–C). At this time, all *cia* alleles exhibited wild-type numbers of circulating red cells (Fig. 1D–F). As development proceeded, *cia^{tu25f}* embryos continued to show less severe hypochromia than the other alleles (Fig. 1G–I). Embryos of each *cia* allele exhibited a decrease in total red cell number compared with wild-type by 72 hpf; *cia^{tu25f}* had the least severe anemia (50% of wild-type cell numbers); both *cia^{hp327}* and *cia^{tu089}* had a more severe anemia (30% of wild type), and *cia^{hs019}* had the most severe anemia (<10% of wild type) (Fig. 1J–L). *cia^{tu25f}* and *cia^{tu089}* were both homozygous viable, while *cia^{hp327}* and *cia^{hs019}* were lethal between 7 and 10 days post fertilization (dpf). Hematopoietic commitment and early differentiation were found to progress normally in *cia*, as the gene expression of *scl*, *gatal* and various embryonic globins were indistinguishable from wild type until 36 hpf; however, at 72 and 96 hpf, *gatal* expression persisted in *cia* circulating cells, suggesting a block or delay in their differentiation (data not shown). By contrast, examination of lymphoid and myeloid cell gene expressions found no differences in *cia* mutants (data not shown). These analyses suggested that *cia* had a specific defect in late-stage erythroid differentiation.

The viable *cia^{tu25f}* and *cia^{tu089}* alleles survived to adulthood without symptoms of prolonged anemia, such as growth retardation, pallor or cardiomegaly. However, examination of peripheral blood from *cia^{tu25f}* and *cia^{tu089}* adults revealed that definitive erythrocytes in these animals were hypochromic and microcytic. Additionally, an increased number of undifferentiated red cells was present in peripheral circulation

Fig. 1. Characterization of the embryonic blood phenotype in *cia*.

(A–L) Ventral views of the anterior region of embryos. (A–C, G–I) Whole-mount *o*-dianisidine staining of wild-type and *cia* embryos.

Compared with wild type at 36 hpf (A), *cia^{hp327}* (B) (shown as representative of *cia^{hs019}* and *cia^{tu089}* at all stages) lack hemoglobinized erythrocytes, while *cia^{tu25f}* (C) manifest a moderate decrease. At 72 hpf, circulating hemoglobinized erythrocytes are still absent in *cia^{hp327}* (H) and a moderate decrease is again observed in *cia^{tu25f}* (I) compared with wild type (G). (D–F, J–L) Whole-mount RNA in-situ hybridization for *βe1 globin* in wild-type and *cia* embryos. (D–F) At 36 hpf, *cia* embryos are indistinguishable from wild type, while the onset of anemia in *cia* is apparent at 72 hpf, with *cia^{hp327}* (K) possessing less than approximately 30% of cells compared with wild type (J), and *cia^{tu25f}* (L) exhibiting an approximate 50% decrease in erythrocytes.



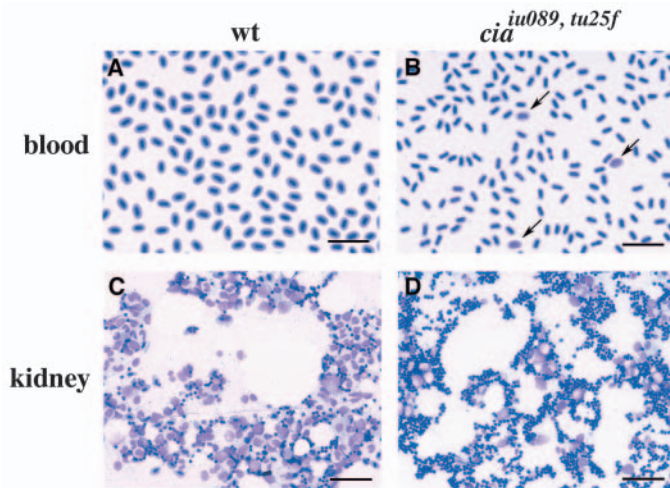


Fig. 2. Adult blood characterization in *cia^{tu25f}* and *cia^{iu089}*. (A,B) Wright-Giemsa staining of peripheral blood collected from wild-type zebrafish adults and *cia* shows that mutant red blood cells are visibly microcytosed, and reveals the presence of undifferentiated cells (arrows) in circulation. (C,D) Kidney samples from wild-type and *cia* adults shows an increased number of erythroid precursors of *cia* mutants, as well as markedly increased cellularity. Scale bars: 20 μ m in A,B; 40 μ m in C,D.

(Fig. 2A,B). Kidney smears from *cia^{tu25f}* and *cia^{iu089}* adults showed an increase in erythroblasts present in the kidney marrow, as well as hypercellularity when compared with wild-type adult zebrafish (Fig. 2C,D). These data demonstrate that the *cia* genetic lesion also perturbs adult erythropoiesis.

Zebrafish *tfr1a* is the gene defective in *cia*

To gain further insight into this phenotype, we isolated the *cia* gene by a candidate cloning strategy. Using bulk segregant analysis, the *cia* gene was mapped to linkage group (LG) 2. Linkage analysis of 996 meioses placed the *cia* locus between SSLP markers z4300 and z7634, approximately 2.7 cM north of the closest genetic marker, z7634 (Fig. 3). Examination of expressed sequence tags (ESTs) in this region revealed synteny to human chromosome 3, which suggested that Tfr1 was a candidate for *cia* (Fig. 3A). Degenerate PCR was used to isolate a 329 bp *tfr1*-like zebrafish clone. Using this fragment to screen a zebrafish kidney cDNA library, 29 partial clones were isolated. Sequencing of the library clones revealed that they encoded a different *tfr1*-like gene, which we designated as *tfr1b*. Radiation hybrid mapping of both zebrafish *tfr1* genes placed *tfr1a* (the 329 bp clone) within the prospective *cia* locus on LG2, while *tfr1b* was mapped to a location on LG24 (Fig. 3A). Interestingly, examination of ESTs on the LG24 radiation hybrid panel in the vicinity of *tfr1b* also detected synteny to human chromosome 3 (Fig. 3A). This led us to speculate that teleosts had undergone a duplication of the *tfr1* locus during the course of evolution. Comparative genomic analysis among vertebrates has strongly supported the hypothesis that the teleost lineage underwent a genome duplication event after the divergence of teleosts and tetrapods (Amores et al., 1998; Gates et al., 1999; Postlethwait et al., 1998; Woods et al., 2000). It has been estimated that at least 20% of the duplicated genes were maintained during subsequent teleost evolution

(Postlethwait et al., 2000). With this in mind, in combination with the synteny we observed between the human *Tfr1*, zebrafish *tfr1a* and zebrafish *tfr1b* loci, we hypothesized that *tfr1a* and *tfr1b* represented the outcome of an ancestral teleost Tfr1 duplication.

We isolated the full-length cDNAs of zebrafish *tfr1a* and *tfr1b* by a combination of 5' and 3' rapid amplification of cDNA ends (RACE) PCR. Sequence comparison of the full-length clones revealed that the zebrafish Tfr1a and Tfr1b predicted peptides are 43.5% identical to each other, and respectively 39% and 35% identical to human Tfr1; comparison of the helical domain that is responsible for Tfr dimerization and Tf binding (Aisen, 2004) showed that they shared 44% and 49% identity with human Tfr1, respectively (Fig. 3B and data not shown). Blast search of the pufferfish genome similarly showed two Tfr1-like predicted proteins, further supporting an ancestral teleost *tfr1* duplication event. Phylogenetic comparison among known vertebrate Tfr genes revealed that zebrafish and pufferfish *tfr1*-like genes were in fact most closely related, and clustered separately from the *tfr1* of higher vertebrates (Fig. 3C). During these analyses, we discovered that zebrafish also possessed an ortholog to mammalian *tfr2*. We isolated the full-length cDNA of zebrafish *tfr2*, and found it clustered with greatest similarity to known human and mouse *tfr2* (Fig. 3B,C).

To determine whether mutations in *tfr1a* were present in the various *cia* alleles, RT-PCR was used to obtain full-length cDNA clones of *tfr1a* from embryos of each allele. Each *cia* allele was found to harbor a mutation in either the *tfr1a* open reading frame or a conserved splice site (Fig. 3B). Sequence analysis of *tfr1a* in *cia^{hp327}* identified a T-to-A transversion at nucleotide +1889 that results in an I→N missense mutation at codon 630. *cia^{hs019}* were found to have a G-to-A transition at nucleotide +1970 that causes a G→D missense mutation at codon 657. The residues mutated in *cia^{hp327}* and *cia^{hs019}* are both located in the Tfr1a regions of the helical domain involved in Tf binding (Buechegger et al., 1996; Cheng et al., 2004; Lawrence et al., 1999). Mutagenesis studies have further localized the Tf/Tfr binding interface to include a conserved RGD sequence, and mutation of the glycine in particular severely abrogates Tf binding (Dubljevic et al., 1999; Giannetti et al., 2003; Liu et al., 2003; West et al., 2001). As the *cia^{hs019}* mutation occurs at this particular glycine, we predict it may directly eliminate Tf binding, although this tripeptide in Tfr1a is replaced by QGS residues. The residue mutated in *cia^{hp327}* is located in α helix 1 of the helical domain, adjacent to a lysine residue critical for Tf binding, and may similarly disrupt interaction with the ligand (Giannetti et al., 2003; Liu et al., 2003). We found *cia^{tu25f}* possessed a G-to-A nucleotide transition at the exon 13 splice donor site that results in inclusion of a 90 bp intron with a premature stop codon, which eliminates the entire Tfr1 helical domain as well as 94 residues (approximately 30%) of the protease domain. RT-PCR of *tfr1a* from *cia^{tu25f}* detected the presence of both the wild-type *tfr1a* cDNA and the mis-spliced variant (data not shown). This was consistent with the *cia^{tu25f}* hypomorphic phenotype, as it suggests that to some extent, *cia^{tu25f}* are capable of synthesizing normal Tfr1a. Lastly, we found *cia^{iu089}* had a T-to-C transition at nucleotide +946, with a resulting F→L mis-sense mutation at codon 316. The F316 residue is located on an apical domain loop that is altered in conformation upon Tfr ligand binding,

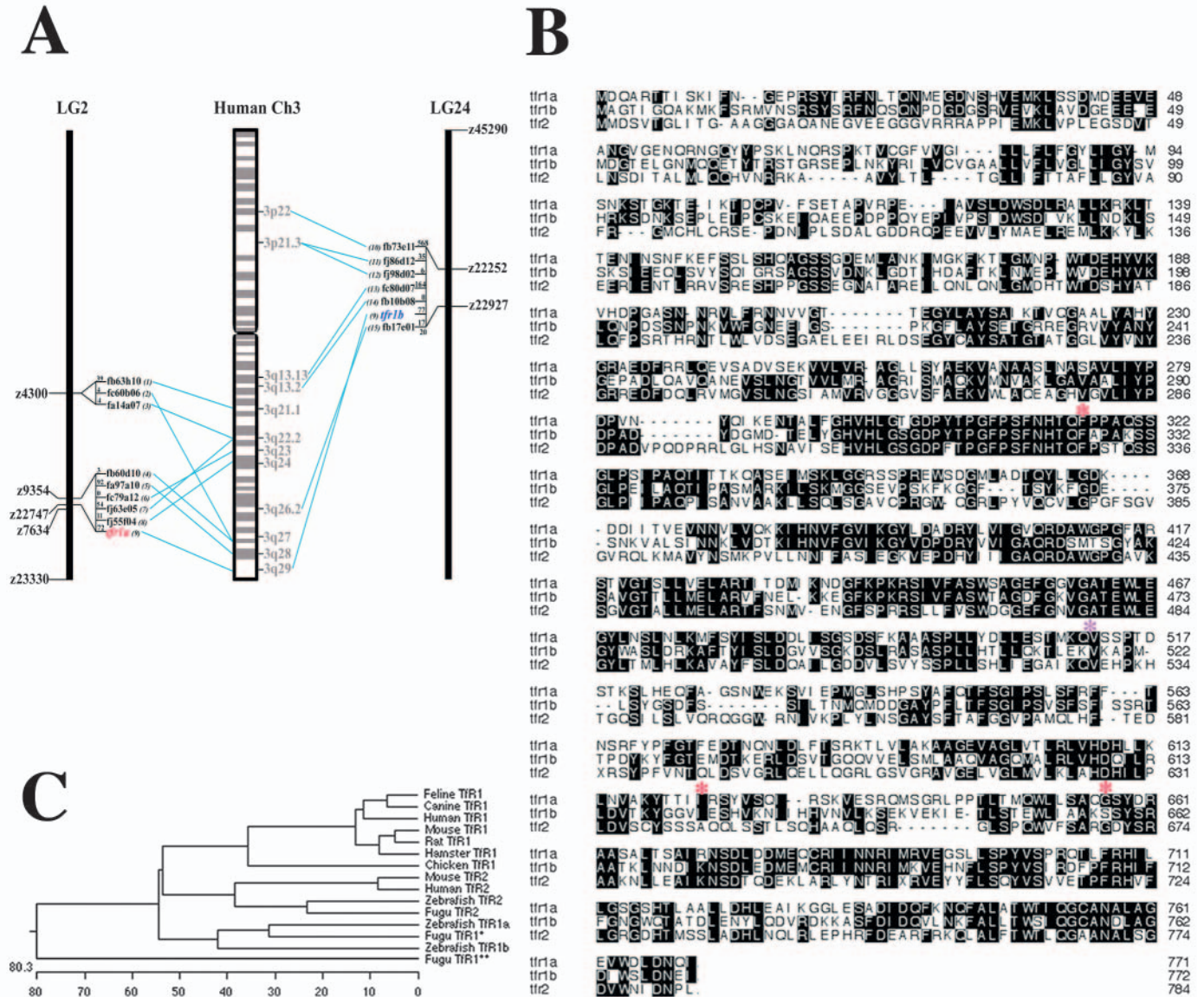


Fig. 3. *tfr1a* is the defective gene in *cia*. (A) (left) Radiation hybrid map of zebrafish LG 2 showing placement of *tfr1a*; (middle) map of human chromosome 3; (right) map of zebrafish LG24 showing the RH map position of *tfr1b*. Syntenic ESTs are shown, with corresponding human orthologs annotated as follows: (1) TF, (2) EIF4G1, (3) ATP1B3, (4) AHSB, (5) AP2M1, (6) LOC51714, (7) EPHB1, (8) CHST2, (9) FTRC, (10) AXUD1, (11) ORCTL3, (12) HYA22, (13) NP25, (14) FLJ1342, (15) EIF5A2. (B) Amino acid alignment of the zebrafish *tfr1a*, *tfr1b*, and *tfr2*; dark shading indicates identical residues, asterisks mark the location of the *cia*^{hp327}, *cia*^{hs019}, *cia*^{iu089} and *cia*^{tu25f} mutations. (C) A phylogenetic tree of the Tfr amino acid sequences reveal divergence between teleost and tetrapod Tfr1 family members, and conservation between known vertebrate Tfr2 proteins. The MegAlign application in DNASTar software was used for alignment and construction of the phylogenetic tree.

and although a mutation in this loop may cause its local destabilization, it is not clear what the precise consequence might be for overall Tfr function.

We next ascertained the expression pattern of each zebrafish *tfr1* during embryogenesis. Whole-mount in-situ hybridization of zebrafish embryos showed *tfr1a* to be highly expressed in the developing blood, as marked by β 1 globin expression (Fig. 4A-H). *tfr1a* expression was first detected at 12 hpf in the ventral mesoderm, which converges to form the hematopoietic intermediate cell mass, the zebrafish intraembryonic blood island (data not shown). Blood-specific expression of *tfr1a* was maintained until 36 hpf in circulating

primitive erythrocytes. By contrast, *tfr1b* was found to be expressed ubiquitously throughout embryogenesis (Fig. 4C,F,I). Notably, expression was not elevated above the level of ubiquitous expression in either developing or circulating primitive erythrocytes.

To provide further evidence that a defect in *tfr1a* was responsible for the *cia* phenotype, we used morpholino (MO) antisense oligonucleotides to inhibit either *tfr1a* mRNA translation or splicing and effect a transient genetic knockdown (Nasevicius and Ekker, 2000). MOs were designed to the *tfr1a* start site (MO1) and to the *tfr1a* exon 13 splice donor (MO2). When injected into wild-type zebrafish embryos, both *tfr1a*

MO1 and MO2 prevented erythrocyte hemoglobin synthesis, resulting in embryos that displayed hypochromic erythrocytes that were *o*-dianisidine negative (Fig. 5A-C and data not shown). Co-injection of *tfr1a* mRNA was able to rescue the hemoglobin defect in 18% (30/167) of the animals injected with *tfr1a* MO1, demonstrating that the phenotype in *tfr1a* morphant embryos was specific (Fig. 5D).

Lastly, we confirmed the ability of *tfr1a* to rescue hemoglobin production in *cia* mutants by overexpression. Wild-type *tfr1a* mRNA was injected into *cia^{iu089}* homozygous embryos, resulting in a partial rescue of *o*-dianisidine positive cells at the 36-40 hpf stage (Fig. 5E; Table 1). From these experiments we concluded that mutations in *tfr1a* were causal for the *cia* phenotype.

Provision of iron rescues *cia* hypochromia

To demonstrate the requirement of *tfr1a* for iron uptake in *cia* erythroid precursors, we attempted to rescue embryonic hypochromia with two methods of iron delivery. First, we tested whether injection of *cia^{iu089}* embryos with iron-dextran at the 1-cell stage could remedy their hypochromia. We

Table 1. Rescue of hemoglobin synthesis in *cia^{iu089}* with assorted *tfr* family members

Injected cRNA	Partial rescue by <i>o</i> -dianisidine stain	Overall percentage
Zebrafish <i>tfr1a</i>	40/164	24
Zebrafish <i>tfr1b</i>	54/196	27
Mouse <i>tfr1</i>	37/222	17
Mouse <i>tfr2</i>	45/164	27

hypothesized that by overloading the embryo cytoplasm with iron-dextran at the 1-cell stage, we would deposit a supply of usable iron to be distributed during subsequent embryo cleavage, such that the cytoplasm of all cells would directly receive iron and circumvent the need for *tfr1a* function. We found that injection of 1-cell staged *cia^{iu089}* with iron-dextran robustly rescued hypochromia at 40 hpf (138/297; 46%) (Fig. 6A). By facilitating the delivery of cytoplasmic iron to erythrocytes, we have demonstrated that the biochemical function of Tfr1a is to facilitate iron uptake across the zebrafish red cell membrane.

Second, previous work had found that intravenous injection of iron-dextran at 48 hpf rescued hemoglobin production over subsequent days in zebrafish mutants with inadequate iron present in circulation if the primitive erythrocytes were competent to uptake and utilize iron (Donovan et al., 2000). Thus we used intravenous injection of iron-dextran to assess whether (excess) available iron would ameliorate the *cia* hemoglobin defect. We anticipated that intravenous iron would not rescue defective hemoglobinization in *cia*, due to the

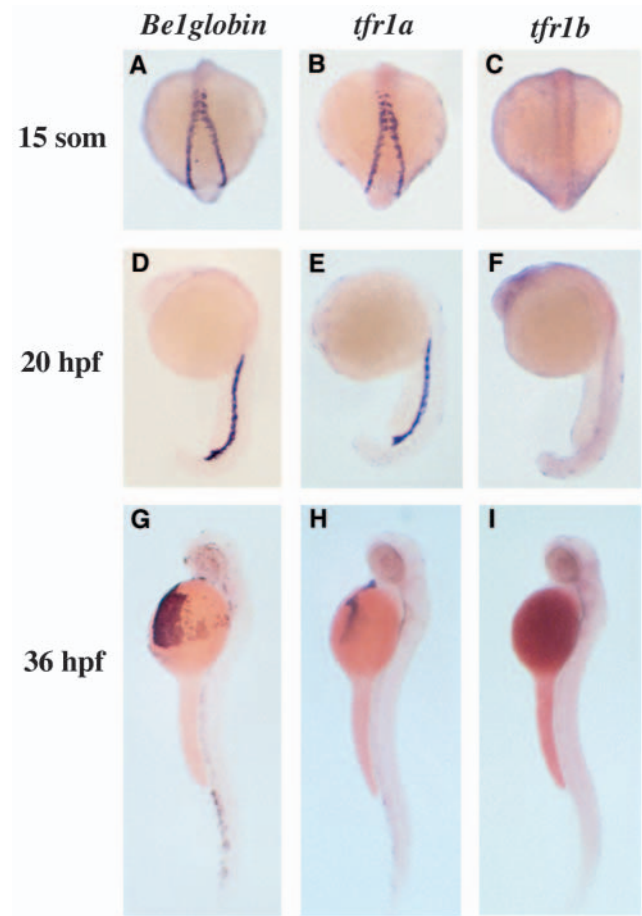


Fig. 4. Expression patterns of zebrafish *tfr1a* and *tfr1b* during embryogenesis. Whole-mount RNA in-situ hybridization for *tfr1a* (B,E,H) shows an expression pattern restricted to the hematopoietic intermediate cell mass and later circulating blood, identical to that of β 1 globin (A,D,G), shown at 15 somites, 20 hpf, and 36 hpf. By contrast, the expression of *tfr1b* (C,F,I) at these timepoints is ubiquitous.

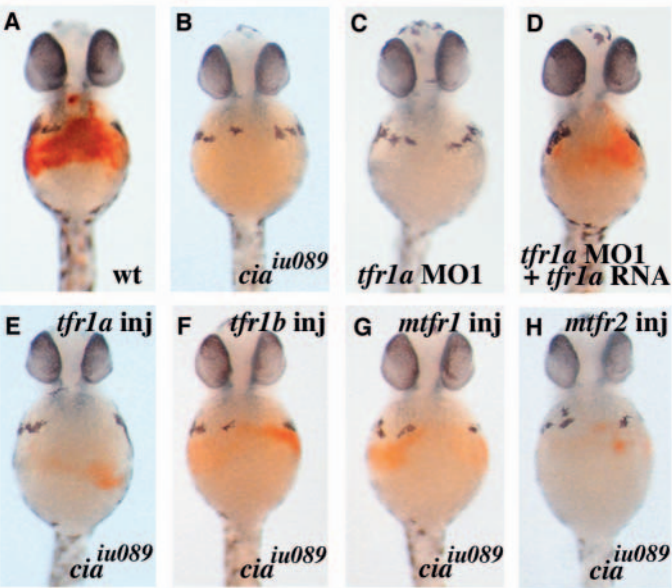


Fig. 5. *tfr1a* is required for erythrocyte hemoglobin production, but multiple Tfr family members can compensate for loss of *tfr1a* in *cia*. (A-H) Ventral views of the anterior region of *o*-dianisidine stained embryos at 40 hpf. (A) Uninjected wild type. (B) Uninjected *cia^{iu089}*. (C) Wild-type embryo injected with *tfr1a* MO1 did not exhibit hemoglobinized erythrocytes. (D) Wild-type embryo co-injected with *tfr1a* MO1 and *tfr1a* cRNA was partially rescued. (E-H) *cia^{iu089}* embryos injected with cRNA of *tfr1a* (E), *tfr1b* (F), mouse *tfr1* (G), and mouse *tfr2* (H) all exhibited partial rescue of hypochromia.

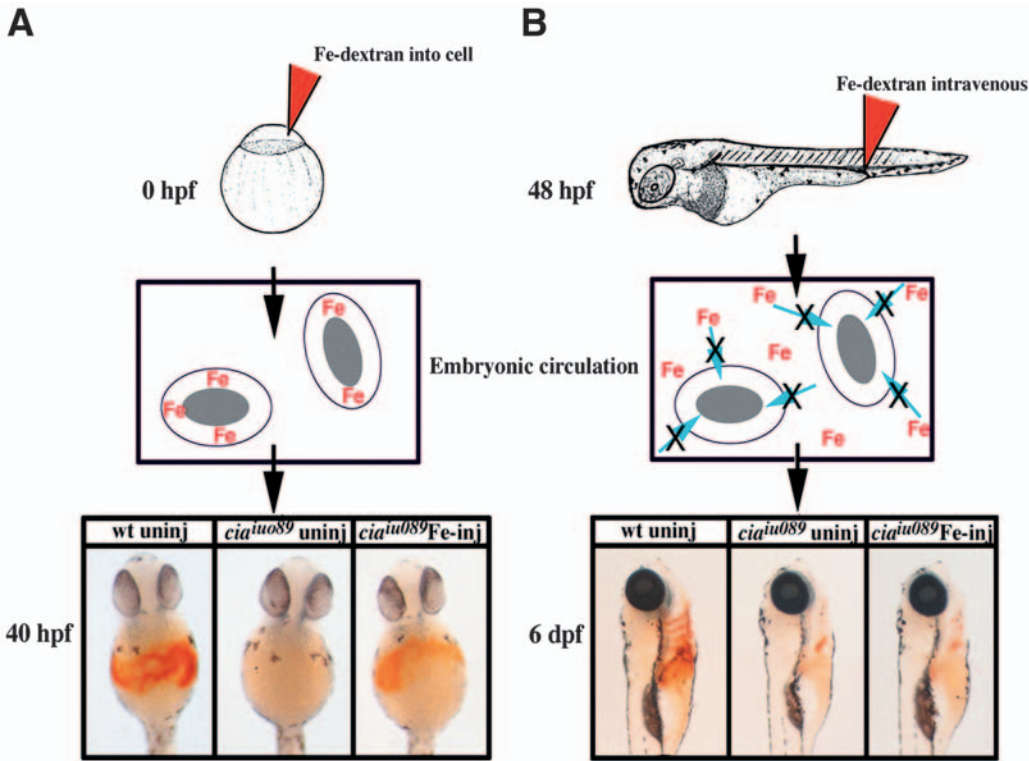


Fig. 6. Provision of iron-dextran to *cia* erythroid precursors bypasses the requirement for *tfr1a* function. (A) (top) Injection of iron-dextran at the 1-cell stage causes (middle) direct delivery of a cytoplasmic iron to all cells in the embryo, resulting (bottom) in the rescue of hypochromia in 40 hpf *cia^{iu089}* embryos. (B) (top) Intravenous injection of iron-dextran into 48 hpf *cia^{iu089}* places (middle) excess iron into embryonic circulation, but this iron cannot be obtained by *cia* red cells due to a block at the level of iron acquisition across the cell membrane, resulting (bottom) in the failure of this iron provision to remedy *cia* hypochromia.

loss of Tfr1a function. Injection of iron-dextran into the circulation of *cia^{iu089}* or *cia^{tu25f}* at 48 hpf was in fact unable to rescue hypochromia when assessed over subsequent days (0/87; 0%) (Fig. 6B). The failure of this late-stage iron injection to rescue *cia* hemoglobin synthesis shows the inability of the *cia* erythrocytes to acquire iron when the circulation had been saturated with a usable iron source. In addition, this result highlights that erythrocytes only acquire appreciable cellular iron levels through the function of Tfr1a.

Zebrafish *tfr1b* is used for iron uptake by non-hematopoietic tissues

Based on the in-situ hybridization, as well as RT-PCR analyses from embryos between 24 hpf and 6 dpf, it was evident that *tfr1b* was expressed throughout embryogenesis (Fig. 4 and data not shown). To investigate the role of *tfr1b* during development, we used antisense MOs to evaluate loss of *tfr1b* function. In particular, we were interested in whether abrogation of Tfr1b would affect hemoglobinization during erythroid cell differentiation. A MO designed against the *tfr1b* translational start site (MO1) was injected into wild-type zebrafish embryos at the 1-cell stage and the embryos were examined throughout development. At 18-24 hpf, *tfr1b* MO1-injected animals exhibited brain necrosis and growth

delay. By 36-48 hpf, embryos were still developmentally delayed, and could be grouped into three classes according to their overall growth progression and the severity of their nervous system necrosis (Table 2, Fig. 7). Class I injected animals (7.8%) exhibited a moderate growth delay in comparison with uninjected wild-type embryos (Fig. 7A-D). Class II injected embryos (87.5%) displayed severe growth retardation, being much smaller with a markedly curved trunk and tail (Fig. 7E,F). Class III injected embryos (4.7%) included the morphants with extreme growth retardation (Fig. 7G,H). All Class II and III affected morphants died before 5 dpf. Despite this, all *tfr1b* morphant groups underwent normal hemoglobinization, with visibly red blood in circulation and *o*-dianisidine concentrations indistinguishable from uninjected wild-type siblings. Similar results were observed with co-injection of the MOs targeted to the splice donor and acceptor sites at the junction between exons 1 and 2 (data not shown).

To exclude the possibility that the *tfr1b* MO phenotype was due to MO toxicity, we attempted to rescue the generalized growth defects and nervous tissue necrosis with concomitant *tfr1b* mRNA overexpression. Co-injection of *tfr1b* MO1 and *tfr1b* cRNA into 1-cell stage wild-type embryos resulted in a greater number of Class I animals (30.6%) (Fig. 7I,J; Table 2). The ability of *tfr1b* overexpression to ameliorate the combination of growth and necrosis effects of *tfr1b* MO1 demonstrated that the observed embryo phenotype was reflective of *tfr1b* loss of function. From these experiments, we conclude that zebrafish *tfr1b* is not necessary for erythroid iron uptake. The *tfr1b* MO phenotype and the ubiquitous *tfr1b* expression pattern suggest that Tfr1b is most likely used by all non-erythroid cells for iron assimilation.

Table 2. Phenotypic classes of *tfr1b* MO1-injected embryos

	<i>tfr1b</i> MO1, 1.25 mM	<i>tfr1b</i> MO1, 1.25 mM + <i>tfr1b</i> RNA
Class I	15 (7.8%)	86 (30.6%)
Class II	168 (87.5%)	150 (53.4%)
Class III	9 (4.7%)	45 (16.0%)

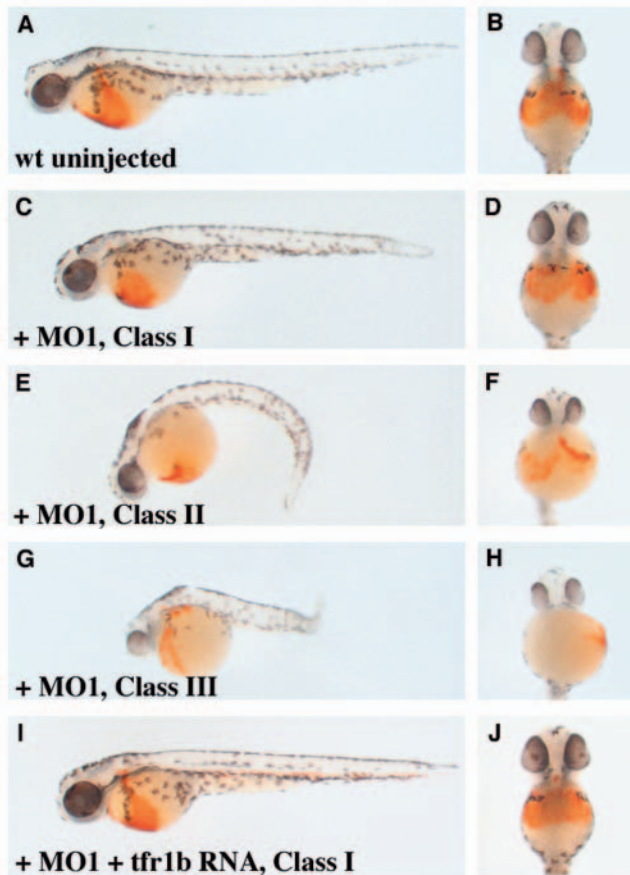


Fig. 7. Functional analysis of zebrafish *tfr1b* using morpholinos. (A,C,E,G,I) All show lateral views of 48 hpf *o*-dianisidine stained embryos, anterior to the left, with (B,D,F,H,J) showing ventral views of the same embryos. (A) Uninjected wild type. (C-H) Wild-type embryos injected with *tfr1b* MO1 exhibit three categories of phenotypic classes: (C,D) Class I embryo; (E,F) Class II embryo; and (G,H) Class III embryo. (I,J) Embryo co-injected with *tfr1b* MO1 and *tfr1b* cRNA.

Multiple Tfr genes are sufficient to rescue hypochromia in *cia*

We next determined if *tfr1b* could compensate for the loss of *tfr1a* function in *cia* erythrocytes. We overexpressed *tfr1b* in *cia^{iu089}* mutants and found that hemoglobin production was partially rescued in 27% of animals injected (Fig. 5F; Table 1). The number of *cia^{iu089}* rescued and the degree of rescue were similar to that observed when *tfr1a* was overexpressed. These results confirm that Tfr1b functions to deliver cellular iron. We also examined expression of *tfr1b* in *cia* mutants to assess if its expression might be altered, and hence partly accountable for the homozygous viability of *cia^{iu089}* and *cia^{tu25f}*. However, we detected no changes in *tfr1b* expression in any *cia* allele by whole-mount in-situ hybridization (data not shown). Thus, taken together with the morpholino data, this shows that while *tfr1b* is capable of iron delivery into erythrocytes, it is not normally utilized by developing erythroid cells.

As Tf receptors are conserved in structure throughout vertebrate evolution, we wondered if multiple family members would be able to rescue *cia* when similarly overexpressed in

the embryo. In support of a common biochemical function, we found that the overexpression of mouse *tfr1* mRNA partially rescued hemoglobin synthesis in 17% of *cia^{iu089}* embryos (Fig. 5G, Table 1). Again, the number of *cia* embryos rescued and quantity of cells per embryo in which hemoglobin was detected were similar to the overexpression experiments conducted with *tfr1a* and *tfr1b*. Although the function of Tfr2 in body iron metabolism has yet to be elucidated, mammalian Tfr2 is capable of binding and transporting Tf-bound iron in vitro (Kawabata et al., 1999; Kawabata et al., 2001; West et al., 2000). Based on these data, we tested if overexpression of Tfr2 would rescue hemoglobin production in *cia*. Injection of *cia^{iu089}* mutants with mouse *tfr2* mRNA at the 1-cell stage partially rescued hypochromia in 27% of mutants (Fig. 5H; Table 1). Thus mammalian Tfr2 was also able to compensate for loss of *tfr1a* function in erythroid cells. This series of Tfr overexpression experiments suggests that the presence of any number of known Tf receptors on a differentiating erythrocyte can facilitate iron uptake adequate for the production of hemoglobin.

Discussion

Our study of the *cia* mutant illustrates that a defect in *tfr1a* function specifically causes a hypochromic, microcytic anemia in zebrafish. We have shown that *tfr1a* is required for normal hemoglobin synthesis during zebrafish erythropoiesis. Our results demonstrate that *tfr1a* is a transferrin receptor exclusively used by erythrocytes, since *tfr1a* is highly expressed in the developing blood, each *cia* allele exhibits a blood-specific phenotype, and transient knockdown of *tfr1a* using morpholinos resulted in hypochromic blood in otherwise normal embryos. The injection of iron-dextran at the 1 cell-stage rescued the hemoglobin defect in *cia* embryos, showing that loss of *tfr1a* prevents erythrocytes from acquiring iron. In all other respects, *cia* erythrocytes are capable of normal hemoglobin production. Thus the biochemical role of zebrafish *tfr1a* to mediate cellular iron acquisition is conserved with that of vertebrate Tfr1s. In contrast to *tfr1a*, zebrafish *tfr1b* is not required for erythropoiesis. Rather, *tfr1b* function is indispensable for proper growth and development of non-hematopoietic tissues in the embryo. The sum of zebrafish Tfr1a and Tfr1b functions equate to that of the single mammalian Tfr1. Although other pathways of cellular iron delivery have been characterized, they are not sufficient to compensate for the role of *tfr1a* in erythropoiesis or the role of *tfr1b* during ontogeny.

Functional equivalence among vertebrate Tfr genes in vivo

The overexpression of several Tfr genes in *cia* embryos was shown to attenuate the *cia* hypochromic phenotype. These results illustrate that when expressed in differentiating erythroid cells, a number of Tf receptors are capable of mediating iron uptake sufficient for hemoglobin biosynthesis. Our data specifically show the functional equivalence between zebrafish *tfr1a*, zebrafish *tfr1b*, mouse *Tfr1*, and mouse *Tfr2* in the developing zebrafish. It is particularly noteworthy that *cia* could be rescued with mouse Tfr2, as this is the first in-vivo illustration of Tfr2 facilitating erythroid iron uptake. This finding emphasizes that functional differences between

mammalian Tfr1 and Tfr2 result from differences in the spatiotemporal expression of these respective genes.

Complementary roles of the zebrafish *tfr1* duplicate genes during embryogenesis

The phenomenon of an erythroid-specific transferrin receptor in zebrafish is most likely explained by a teleost genome duplication event postulated to have happened following the split between teleost and tetrapod lineages (Amores et al., 1998; Gates et al., 1999; Postlethwait et al., 1998; Woods et al., 2000). Based on the presence of gene duplicates discovered in multiple teleosts, including zebrafish, pufferfish and medaka, the genome duplication is predicted to have occurred at least 100 million years ago in a teleost ancestor that pre-dates the radiation of teleosts (Amores et al., 1998; Aparicio et al., 1997; Christoffels et al., 2004; Gates et al., 1999; Naruse et al., 2000; Santini and Tyler, 1999; Taylor et al., 2003; Wittbrodt et al., 1998). Our finding that the summation of zebrafish Tfr1a and Tfr1b functions equate to that of mammalian Tfr1 is consistent with the subfunctionalization model of gene duplicate preservation, in which gene copies retain part of the original gene's function (Force et al., 1999; Ohno, 1970; Prince and Pickett, 2002; Zhang, 2003). Common with other examples of subfunctionalization, the respective expression patterns of the *tfr1a* and *tfr1b* have diverged, such that together they recreate the expression of the single ancestral gene, even though in this case the proteins have interchangeable biochemical functions (Bruce et al., 2001; Chiang et al., 2001; de Martino et al., 2000; Dorsky et al., 2003; Lister et al., 2001; Nornes et al., 1998; Oates et al., 1999; Pfeffer et al., 1998). We speculate that non-overlapping *tfr1a* and *tfr1b* expression was made possible by the evolution of different sets of regulatory elements for each duplicate. Future work in defining the promoter elements of *tfr1a* and *tfr1b* will better characterize the potential differences in the regulation and developmental expression of these genes.

Zebrafish as a vertebrate model to study the metabolism of iron and other essential metals

As part of our assessment of *tfr1a* function in erythropoiesis, we developed a means to distinguish between cell extrinsic and intrinsic defects in iron utilization. We utilized a previously characterized method of zebrafish intravenous iron-dextran injection to determine if low plasma iron was a factor in the failure of *cia* erythrocytes to hemoglobinize normally (Donovan et al., 2000). In this assay, the ability to rescue hemoglobin synthesis with intravenously-supplied iron demonstrates that the erythrocytes are fully capable of iron uptake, intracellular trafficking and metabolism; in direct contrast, the inability to rescue indicates that the presence of a defect(s) intrinsic to the mechanism of cellular iron uptake or utilization in erythrocytes is present. Our de-novo method of iron-dextran injection at the 1-cell stage then serves to test whether developing erythrocytes can traffic and metabolize intracellular iron subsequent to iron uptake. With this assay, we believe that provision of excess iron to the embryo cytoplasm before the onset of cleavage acts to bypass the later necessity for erythroid iron internalization, because all cells in the embryo have been saturated with an excess of usable iron. This novel combination of iron-dextran injection assays is a valuable tool that can now be employed to categorize

hypochromic mutants with unknown gene defects currently being studied in our laboratory.

We found it surprising that injection of iron-dextran at the 1-cell stage was relatively non-toxic to the embryo, and we expect this forecasts broader applicability of similar assays. Single cell injection of any number of conjugated trace metals, such as copper or zinc, could be utilized to investigate their function and metabolism in a developmental setting. As we have done, the method could be applied to track various maternal yolk storage components, and could be applied to characterize the defect(s) in genetic mutants. Zebrafish present a unique opportunity to better understand the transit and utilization of iron and other metals during embryogenesis, and such studies in genetic mutants will enable investigation of the pathophysiology of numerous disease states.

In recent years, elucidation of the defects in several zebrafish with hypochromic anemia, in conjunction with the ongoing development of assays to understand their biology, have made significant contributions to the understanding of vertebrate iron metabolism. In this report we have presented evidence that *cia* represents a specific defect in erythrocyte iron uptake due to an ancestral duplication of the teleost *tfr1* locus. Thus *cia* provide a model to further define the role of Tfr1 in erythropoiesis without a panorama of complicating tissue defects. Furthermore, the zebrafish system provides the ability to implement targeted genetic and chemical screens that could identify additional pathways with a role in the maintenance of iron homeostasis.

We thank members of the Zon laboratory for review of this manuscript, D. Giarla for excellent administrative support, V. Sellers for the gift of mouse *Tfr1* and *Tfr2* clones, and A. Giannetti and P. Bjorkman for helpful discussion of Tfr1 functional domains. R.A.W. is supported by Hematology Training Grant, T32 HL07623, is a Harvard University Fellow of the Albert J. Ryan Foundation, and thanks G. Wingert and V. Wingert for their tremendous love and support. L.I.Z. is an Investigator of the Howard Hughes Medical Institute. This work was supported by HHMI and NIH grants HL073427, DK53298 and HL32262.

Tübingen 2000 Screen Consortium

F. Bebbler van, E. Busch-Nentwich, R. Dahm, H. G. Frohnhofer, H. Geiger, D. Gilmour, S. Holley, J. Hooge, D. Jülich, H. Knaut, F. Maderspacher, C. Neumann, T. Nicolson, C. Nüsslein-Volhard, H. Roehl, U. Schönberger, C. Seiler, C. Söllner, M. Sonawane, A. Wehner, C. Weiler and B. Schmidt at the Max-Planck-Institut für Entwicklungsbiologie, Spemannstrasse 35, 72076 Tübingen, Germany.

U. Hagner, E. Hennen, C. Kaps, A. Kirchner, T. I. Koblezek, U. Langheinrich, C. Metzger, R. Nordin, M. Pezzuti, K. Schlombs, J. deSantana-Stamm, T. Trowe, G. Vacun, A. Walker and C. Weiler at Artemis Pharmaceuticals/Exelixis Deutschland GmbH, Neurather Ring 1, S51063 Köln, Germany.

References

- Aisen, P. (2004). Molecules in focus: Transferrin receptor 1. *Int. J. Biochem. Cell Biol.* **36**, 2137-2143.
- Amores, A., Force, A., Yan, Y. L., Joly, L., Amemiya, C., Fritz, A., Ho, R. H., Langeland, J., Prince, V., Wang, Y. L. et al. (1998). Zebrafish hox clusters and vertebrate genome evolution. *Science* **282**, 1711-1714.
- Andrews, N. C. (1999). Disorders of iron metabolism. *N. Engl. J. Med.* **341**, 1986-1995.
- Andrews, N. C. (2000). Iron homeostasis: insights from genetics and animal models. *Nat. Rev. Genet.* **1**, 208-217.

- Aparicio, S., Hawker, K., Cottage, A., Mikawa, Y., Zuo, L., Venkatesh, B., Chen, E., Krumlauf, R. and Brenner, S. (1997). Organization of the Fugu rubripes Hox clusters: evidence for continuing evolution of vertebrate Hox complexes. *Nat. Genet.* **16**, 79-83.
- Baker, E., Baker, S. M. and Morgan, E. M. (1998). Characterization of non-transferrin-bound iron (ferric citrate) uptake by rat hepatocytes in culture. *Biochim. Biophys. Acta* **1380**, 21-30.
- Brownlie, A. and Zon, L. I. (1999). The zebrafish as a model system for the study of hematopoiesis. *Bioscience* **49**, 382-392.
- Brownlie, A., Donovan, A., Pratt, S. J., Paw, B. H., Oates, A. C., Brugnara, C., Witkowska, H. E., Sassa, S. and Zon, L. I. (1998). Postional cloning of the zebrafish sauterne gene: a model for congenital sideroblastic anemia. *Nat. Genet.* **20**, 244-250.
- Brownlie, A., Hersey, C., Oates, A. C., Paw, B. H., Falick, A. M., Witkowska, H. E., Flint, J., Higgs, D., Jessen, J., Bahary, N. et al. (2003). Characterization of embryonic globin genes of the zebrafish. *Dev. Biol.* **255**, 48-61.
- Bruce, A. E., Oates, A. C., Prince, V. E. and Ho, R. K. (2001). Additional hox clusters in the zebrafish: divergent expression patterns belie equivalent activities of duplicate hoxB5 genes. *Evol. Dev.* **3**, 127-144.
- Buchegger, F., Trowbridge, I. S., Liu, L. F. S., White, S. and Collawn, J. F. (1996). Functional analysis of human/chicken transferrin receptor chimeras indicates that the carboxy-terminal region is important for ligand binding. *Eur. J. Biochem.* **235**, 9-17.
- Chan, R. Y., Ponka, P. and Schulman, H. M. (1992). Transferrin-receptor-independent but iron-dependent proliferation of variant Chinese hamster ovary cells. *Exp. Cell Res.* **202**, 326-336.
- Cheng, Y., Zak, O., Aisen, P., Harrison, S. C. and Walz, T. (2004). Structure of the human transferrin receptor-transferrin complex. *Cell* **116**, 565-576.
- Chiang, E. F. L., Pai, C. I., Wyatt, M., Yan, Y. L., Postlethwait, J. and Chung, B. C. (2001). Two sox9 genes on duplicated zebrafish chromosomes: expression of similar transcription activators in distinct sites. *Dev. Biol.* **231**, 149-163.
- Christoffels, A., Koh, E. G., Chia, J. M., Brenner, S., Aparicio, S. and Venkatesh, B. (2004). Fugu genome analysis provides evidence for a whole-genome duplication early during the evolution of ray-finned fishes. *Mol. Biol. Evol.* **Mar 10 Epub**.
- deMartino, S., Yan, Y. L., Jowett, T., Postlethwait, J. H., Varga, Z. M., Ashworth, A. and Austin, C. A. (2000). Expression of sox11 gene duplicates in zebrafish suggests the reciprocal loss of ancestral gene expression patterns in development. *Dev. Dyn.* **217**, 279-292.
- Donovan, A., Brownlie, A., Zhou, Y., Shepard, J., Pratt, S. J., Moynihan, J., Paw, B. H., Drejer, A., Barut, B., Zapata, A. et al. (2000). Positional cloning of zebrafish ferroportin1 identifies a conserved vertebrate iron exporter. *Nature* **403**, 776-781.
- Donovan, A., Brownlie, A., Dorschner, M. O., Zhou, Y., Pratt, S. J., Paw, B. H., Phillips, R. B., Thisse, C., Thisse, B. and Zon, L. I. (2002). The zebrafish mutant gene chardonnay (cdy) encodes divalent metal transporter 1 (DMT1). *Blood* **100**, 4655-4659.
- Dorsky, R. I., Itoh, M., Moon, R. T. and Chitnis, A. (2003). Two tcf3 genes cooperate to pattern the zebrafish brain. *Development* **130**, 1937-1947.
- Dubljevic, V., Sali, A. and Goding, J. W. (1999). A conserved RGD (Arg-Gly-Asp) motif in the transferrin receptor is required for binding to transferrin. *Biochem. J.* **341**, 11-14.
- Fleming, R. E., Migas, M. C., Holden, C. C., Waheed, A., Britton, R. S., Tomatsu, S., Bacon, B. R. and Sly, W. S. (2000). Transferrin receptor 2: continued expression in mouse liver in the face of iron overload and in hereditary hemochromatosis. *Proc. Natl. Acad. Sci. USA* **97**, 2214-2219.
- Fleming, R. E., Ahmann, J. R., Migas, M. C., Waheed, A., Koeffler, H. P., Kawabata, H., Britton, R. S., Bacon, B. R. and Sly, W. S. (2002). Targeted mutagenesis of the murine transferrin receptor-2 gene produces hemochromatosis. *Proc. Natl. Acad. Sci. USA* **99**, 10653-10658.
- Force, A., Lynch, M., Pickett, F. B., Amores, A., Yan, Y. L. and Postlewait, J. (1999). Preservation of duplicate genes by complementary, degenerative mutations. *Genetics* **151**, 1531-1545.
- Gates, M. A., Kim, L., Egan, E. S., Cardozo, T., Sirotkin, H. I., Dougan, S. T., Lashkari, D., Abagyan, R., Schier, A. F. and Talbot, W. S. (1999). A genetic linkage map for zebrafish: comparative analysis and localization of genes and expressed structures. *Genome Res.* **9**, 334-347.
- Gelvan, D., Fibach, E., Meyron-Holtz, E. G. and Konijn, A. M. (1996). Ferritin uptake by human erythroid precursors is a regulated iron uptake pathway. *Blood* **88**, 3200-3207.
- Giannetti, A. M., Snow, P. M., Zak, O. and Bjorkman, P. J. (2003). Mechanism for multiple ligand recognition by the human transferrin receptor. *PLoS Biol.* **1**, 341-350.
- Goto, Y., Paterson, M. and Listowski, I. (1983). Iron uptake and regulation of ferritin synthesis by heptoma cells in hormone-supplemented serum-free media. *J. Biol. Chem.* **258**, 5248-5255.
- Haffter, P., Granato, M., Brand, M., Mullins, M. C., Hammerschmidt, M., Kane, D. A., Odenthal, J., van Eeden, F. J., Jiang, Y. J., Heisenberg, C. P. et al. (1996). The identification of genes with unique and essential functions in the development of the zebrafish, Danio rerio. *Development* **123**, 1-36.
- Hentze, M. W., Muckenthaler, M. U. and Andrews, N. C. (2004). Balancing acts: molecular control of mammalian iron metabolism. *Cell* **117**, 285-297.
- Hodgson, L. L., Quail, E. A. and Morgan, E. H. (1995). Iron transport mechanisms in reticulocytes and mature erythrocytes. *J. Cell Physiol.* **162**, 181-190.
- Inman, R. S. and Wessling-Resnick, M. (1993). Characterization of transferrin-independent iron transport in K562 cells. *J. Biol. Chem.* **268**, 8521-8528.
- Kaplan, J., Jordan, I. and Sturrock, A. (1991). Regulation of the transferrin-independent iron transport system in cultured cells. *J. Biol. Chem.* **266**, 2997-3004.
- Kawabata, H., Yang, R., Hiramata, T., Vuong, P. T., Kawano, S., Gombart, A. F. and Koeffler, H. P. (1999). Molecular cloning of transferrin receptor 2. *J. Biol. Chem.* **274**, 20826-20832.
- Kawabata, H., Nakimaki, T., Ikonomi, P., Smith, R. D., Germain, R. S. and Koeffler, H. P. (2001). Expression of transferrin receptor 2 in normal and neoplastic hematopoietic cells. *Blood* **98**, 2714-2719.
- Kimmel, C. B., Ballard, W. W., Kimmel, S. R., Ullman, B. and Schilling, T. F. (1995). Stages of embryonic development of the zebrafish. *Dev. Dyn.* **203**, 253-310.
- Konijn, A. M., Meyron-Holtz, E. G., Fibach, E. and Gelvan, D. (1994). Cellular ferritin uptake: a highly regulated pathway for iron assimilation in human erythroid precursor cells. *Adv. Exp. Med. Biol.* **356**, 189-197.
- Lawrence, C. M., Ray, S., Babyonyshev, M., Galluser, R., Borhani, D. W. and Harrison, S. C. (1999). Crystal structure of the ectodomain of human transferrin receptor. *Science* **286**, 779-782.
- Leimberg, J. M., Konijn, A. M. and Fibach, E. (2003). Developing human erythroid cells grown in transferrin-free medium utilize iron originating from extracellular ferritin. *Am. J. Hematol.* **73**, 211-212.
- Levy, J. E., Jin, O., Fujiwara, Y., Kuo, F. and Andrews, N. C. (1999). Transferrin receptor is necessary for development of erythrocytes and the nervous system. *Nat. Genet.* **21**, 396-399.
- Lister, J. A., Close, J. and Raible, D. W. (2001). Duplicate mitf genes in zebrafish: complementary expression and conservation of melanogenic potential. *Dev. Biol.* **237**, 333-344.
- Liu, R., Guan, J. Q., Zak, O., Aisen, P. and Chance, M. R. (2003). Structural reorganization of the transferrin c-lobe and transferrin receptor upon complex formation: the c-lobe binds to the receptor helical domain. *Biochemistry* **42**, 12447-12454.
- Meyron-Holtz, E. G., Vaisman, B., Cabantchik, Z. I., Fibach, E., Rouault, T. A., Hershko, C. and Konijn, A. M. (1999). Regulation of intracellular iron metabolism in human erythroid precursors by internalized extracellular ferritin. *Blood* **94**, 3205-3211.
- Naruse, K., Fukamachi, S., Mitani, H., Kondo, M., Matsuoka, T., Kondo, S., Hanamura, N., Morita, Y., Hasegawa, K., Nishigaki, R. et al. (2000). A detailed map of medaka, *oryzias latipes*. Comparative genomics and genome evolution. *Genetics* **154**, 1773-1784.
- Nasevicius, A. and Ekker, S. C. (2000). Effective targeted gene 'knockdown' in zebrafish. *Nat. Genet.* **26**, 216-220.
- Ned, R. M., Swat, W. and Andrews, N. C. (2003). Transferrin receptor 1 is differentially required in lymphocyte development. *Blood* **102**, 3711-3718.
- Nornes, S., Clarkson, M., Mikkola, I., Pederson, M., Bardsley, A., Martinez, J. P., Krauss, S. and Johansen, T. (1998). Zebrafish contains two Pax6 genes involved in eye development. *Mech. Dev.* **77**, 185-196.
- Oates, A. C., Brownlie, A., Pratt, S. J., Irvine, D. V., Liao, E. C., Paw, B. H., Dorian, K. J., Johnson, S. L., Postlethwait, J. H., Zon, L. I. et al. (1999). Gene duplication of zebrafish JAK2 homologs is accompanied by divergent embryonic expression patterns: only jak2a is expressed during erythropoiesis. *Blood* **94**, 2622-2636.
- Ohno, S. (1970). *Evolution by Gene Duplication*. Heidelberg, Germany: Springer-Verlag.

- Pfeffer, P. L., Gerster, T., Lun, K., Brand, M. and Busslinger, M.** (1998). Characterization of three novel members of the zebrafish Pax2/5/8 family: dependency of Pax5 and Pax8 expression on the Pax2.1 (noi) function. *Development* **125**, 3063-3074.
- Ponka, P. and Lok, C. N.** (1999). The transferrin receptor: role in health and disease. *Int. J. Biochem. Cell. Biol.* **31**, 1111-1137.
- Postlethwait, J. H., Yan, Y. L., Gates, M. A., Horne, S., Amores, A., Brownlie, A., Donovan, A., Egan, E. S., Force, A., Gong, Z. et al.** (1998). Vertebrate genome evolution and the zebrafish gene map. *Nat. Genet.* **18**, 345-349.
- Postlethwait, J. H., Woods, I. G., Ngo-Hazelett, P., Yan, Y. L., Kelly, P. D., Chu, F., Huang, H., Hill-Force, A. and Talbot, W. S.** (2000). Zebrafish comparative genomics and the origins of vertebrate chromosomes. *Genome Res.* **10**, 1890-1902.
- Prince, V. E. and Pickett, F. B.** (2002). Splitting pairs: the diverging fates of duplicated genes. *Nat. Rev. Genet.* **3**, 827-837.
- Ransom, D. G., Haffter, P., Odenthal, J., Brownlie, A., Vogelsang, E., Kelsh, R. N., Brand, M., van Eeden, F. J. M., Furutani-Seiki, M., Granato, M. et al.** (1996). Characterization of zebrafish mutants with defects in embryonic hematopoiesis. *Development* **123**, 311-319.
- Santini, F. and Tyler, J. C.** (1999). A new phylogenetic hypothesis for the order Tetraodontiformes (Teleostei, Pisces), with placement of the most fossil basal lineages. *Am. Zool.* **39**, 10A.
- Sturrock, A., Alexander, J., Lamb, J., Craven, C. M. and Kaplan, J.** (1990). Characterization of a transferrin-independent uptake system for iron in HeLa cells. *J. Biol. Chem.* **265**, 3139-3145.
- Taylor, J. S., Braasch, I., Frickey, T., Meyer, A. and Van de Peer, Y.** (2003). Genome duplication, a trait shared by 22,000 species of ray-finned fish. *Genome Res.* **13**, 382-390.
- Thompson, M. A., Ransom, D. G., Pratt, S. J., MacLennan, H., Kieran, M. W., Detrich, H. W., 3rd, Vial, B., Huber, T. L., Paw, B., Brownlie, A. J., Oates, A. C., Fritz, A., Gates, M. A., Amores, A., Bahary, N., Talbot, W. S., Her, H., Beier, D. R., Postlethwait, J. H. and Zon, L. I.** (1998). The cloche and spadetail genes differentially affect hematopoiesis and vasculogenesis. *Dev. Biol.* **197**, 248-269.
- Thorstensen, K., Trinder, D., Zak, O. and Aisen, P.** (1995). Uptake of iron from N-terminal half-transferrin by isolated rat hepatocytes. Evidence of transferrin-receptor-independent iron uptake. *Eur. J. Biochem.* **232**, 129-133.
- Trinder, D. and Baker, E.** (2003). Transferrin receptor 2: a new molecule in iron metabolism. *Int. J. Biochem. Cell Biol.* **35**, 292-296.
- West, A. P., Bennett, M. J., Sellers, V. M., Andrews, N. C., Enns, C. A. and Bjorkman, P. J.** (2000). Comparison of the interactions of transferrin receptor and transferrin receptor 2 with transferrin and the hereditary hemochromatosis protein HFE. *J. Biol. Chem.* **275**, 38135-38138.
- West, A. P., Giannetti, A. M., Herr, A. B., Bennett, M. J., Nangiana, J. S., Pierce, J. R., Weiner, L. P., Snow, P. M. and Bjorkman, P. J.** (2001). Mutational analysis of the transferrin receptor reveals overlapping HFE and transferrin binding sites. *J. Mol. Biol.* **313**, 385-397.
- Westerfield, M.** (1993). *The Zebrafish Book*. Eugene, Oregon: University of Oregon Press.
- Wingert, R. A. and Zon, L. I.** (2003). Genetic dissection of hematopoiesis using the zebrafish. In *Hematopoietic Stem Cells* (ed. I. Godin and A. Cumano), pp. 1-18. Georgetown: Texas: Landes Bioscience.
- Wittbrodt, J., Meyer, A. and Scharl, M.** (1998). More genes in fish? *BioEssays* **20**, 511-515.
- Woods, I. G., Kelly, P. D., Chu, F., Ngo-Hazelett, P., Yan, Y. L., Huang, H., Postlethwait, P. H. and Talbot, W. S.** (2000). A comparative map of the zebrafish genome. *Genome Res.* **10**, 1903-1914.
- Yang, J., Goetz, D., Li, J. Y., Wang, W., Mori, K., Setlik, D., Du, T., Erdjument-Bromage, H., Tempst, P., Strong, R. et al.** (2002). An iron delivery pathway mediated by a lipocalin. *Mol. Cell* **10**, 1045-1056.
- Zhang, J.** (2003). Evolution by gene duplication: an update. *Trends Ecol. Evol.* **18**, 292-298.
- Zhang, J., Talbot, W. S. and Schier, A. F.** (1998). Positional cloning identifies zebrafish one-eyed pinhead as a permissive EGF-related ligand required during gastrulation. *Cell* **92**, 241-251.